Available online at www.sciencedirect.com
SCIENCE DIRECT
Remote Sensing of Environment 103 (2006) 81 – 96
Remote Sensing of Environment
www.elsevier.com/locate/rse

Quantifying spatial heterogeneity at the landscape scale using variogram models

S. Garrigues [a,*], D. Allard [b], F. Baret [c], M. Weiss [d]

[a] University of Maryland, NASA's GSFC, Greenbelt, MD, USA
[b] Biométrie, INRA, Avignon, France
[c] Climat Sol Environnement, INRA, Avignon, France
[d] Noveltis, Toulouse, France

Received 18 July 2005; received in revised form 20 March 2006; accepted 22 March 2006

Abstract

The monitoring of earth surface dynamic processes at a global scale requires high temporal frequency remote sensing observations which are provided up to now by moderate spatial resolution sensors. However, the spatial heterogeneity within the moderate spatial resolution pixel biases non-linear estimation processes of land surface variables from remote sensing data. To limit its influence on the description of land surface processes, corrections based on the quantification of the intra-pixel heterogeneity may be applied to non-linear estimation processes. A complementary strategy is to define the proper pixel size to capture the spatial variability of the data and minimize the intra-pixel variability.

This work provides a methodology to characterize and quantify the spatial heterogeneity of landscape vegetation cover from the modeling of the variogram of high spatial resolution NDVI data. NDVI variograms for 18 landscapes extracted from the VALERI database show that the land use is the main factor of spatial variability as quantified by the variogram sill. Crop sites are more heterogeneous than natural vegetation and forest sites at the landscape level. The integral range summarizes all structural parameters of the variogram into a single characteristic area. Its square root quantifies the mean length scale (i.e. spatial scale) of the data, which varies between 216 and 1060 m over the 18 landscapes considered. The integral range is also used as a yardstick to judge if the size of an image is large enough to measure properly the length scales of the data with the variogram. We propose that it must be smaller than 5% of the image surface. The theoretical dispersion variance, computed from the variogram model, quantifies the spatial heterogeneity within a moderate resolution pixel. It increases rapidly with pixel size until this size is larger than the mean length scale of the data. Finally based on the analysis of 18 landscapes, the sufficient pixel size to capture the major part of the spatial variability of the vegetation cover at the landscape scale is estimated to be less than 100 m. Since for all the heterogeneous landscapes the loss of NDVI spatial variability was small at this spatial resolution, the bias generated by the intra-pixel spatial heterogeneity on non-linear estimation processes will be reduced.

Keywords: Spatial heterogeneity; Moderate spatial resolution; Variogram model; Landscape; NDVI; Length scale; Data regularization; Optimal spatial resolution

1. Introduction

Remote sensing observations are relevant to describe land surface processes at the global scale, such as primary production, carbon and water fluxes. However, the monitoring of vegetation functioning requires high temporal frequency data which are provided up to now by moderate spatial resolution sensors with a spatial resolution from few hundred meters (MERIS/ENVISAT, MODIS/TERRA) up to one or few kilometers (VEGETATION/SPOT, SEVIRI/MSG, POLDER/ADEOS, POLDER/PARASOL). At such moderate resolution, the surface observed through the instantaneous field of view of these sensors may be very heterogeneous, because the landscape is a mosaic of objects, such as agricultural fields or vegetation patches, that are often smaller than moderate resolution pixels. Since sensors integrate the radiometric signal over the pixels, intra-pixel spatial heterogeneity information is lost at moderate spatial resolution. Intra-pixel spatial heterogeneity biases non-linear estimation processes of land surface

* Corresponding author. Tel.: +1 301 614 6646.
E-mail address: Sebastien.Garrigues@gsfc.nasa.gov (S. Garrigues).

0034-4257/$ - see front matter © 2006 Elsevier Inc. All rights reserved.
doi:10.1016/j.rse.2006.03.013

variables from moderate spatial resolution sensors (Friedl, 1997; Garrigues, 2004; Hu & Islam, 1997; Raffy, 1994; Tian et al., 2002; Weiss et al., 2000). To limit its influence on the description of land surface processes, a first strategy consists in explicitly taking into account the intra-pixel spatial heterogeneity in non-linear estimation processes (Garrigues et al., in press). This strategy requires quantifying the intra-pixel spatial heterogeneity. A complementary strategy is to define the proper pixel size to capture the spatial variability of the data and minimize the intra-pixel variability (Atkinson, 1995; Curran & Atkinson, 2002; Garrigues, 2004; Marceau et al., 1994; Puech, 1994; Rahman et al., 2003). Therefore, characterizing the landscape spatial heterogeneity may help in designing the spatial resolution for future earth observing missions. Regarding validation field campaigns, the landscape spatial heterogeneity is also an essential information to choose a suitable sampling scheme which captures the spatial scale of the surface property and optimizes the field collection resources (Baret et al., in press; Morisette et al., 2002; Morisette et al., in press; Stein & Ettema, 2003).

To properly characterize the spatial heterogeneity, it must be appropriately defined. A surface property is heterogeneous, if its measurements vary in space (Kolasa & Rollo, 1991). In this paper, spatial heterogeneity is described through two components:

- The *spatial variability* of the surface property over the observed scene.
- The *spatial structures*, also called objects or patches. They repeat themselves independently within the observed scene at a characteristic length scale (i.e. spatial scale) which represents the spatial structure extent. They can be viewed as the typical correlation area (i.e. the typical area of influence) of the surface property. Data are often distributed into independent sets of spatial structures, related to different length scales and spatial variability, being overlaid in the same region. A formal definition of the spatial structures is given in Section 4.3.

In this work the Normalized Difference Vegetation Index (NDVI; Jackson, 1983) is the 'state' variable used to describe the spatial heterogeneity of vegetation cover. Although NDVI is sensitive to soil and atmospheric effects, it is a good indicator of the vegetation amount (Henebry, 1993). Spatial heterogeneity of the measured surface property depends on its observational scale (Bian, 1997; Bierkens et al., 2000; Cao & Lam, 1997; O'Neill et al., 1991; Quattrochi & Goodchild, 1997; Tian et al., 2002). The observational scale is defined by both the geographic extent of the observed scene and the spatial resolution of the data (Bierkens et al., 2000; Cao & Lam, 1997). The geographic extent determines the biological organization level on which the surface property is observed such as the leaves (a few centimeters), the canopy (10 to 100 m), the landscape (100 m to a few kilometers) or the region (about 100 km). When describing the spatial heterogeneity of moderate spatial resolution pixels, the geographic extent corresponds to the landscape level. It is defined in this paper as an area of a few square kilometers (9 to 50 km^2). The spatial resolution of remote sensing data is equal to the nominal pixel size of the image as defined by the size of the sampling step of the sensor at nadir. The sensor system applies a low pass spatial filter to the radiometric signal, characterized by the Point Spread Function (PSF). The spatial support of the PSF defines the size of the actual spatial support of the data which may be larger than the pixel size. In this paper, the PSF effect is neglected. The actual spatial support of the data on which the signal is integrated is thus approximated by the pixel. The combination of the PSF and the sampling step of the sensor determines the minimum size of the objects detected by the sensor. The pixel size must be small enough to characterize the typical length scales of interest. For example, very high spatial resolution images (e.g. CASI, 2.5 m spatial resolution) are necessary to detect objects within the canopy level (like tree crowns in a forest). In this work, the typical length scales of the landscape, such as the extent of an agricultural field, are much larger than the size of the canopy objects. Therefore, high spatial resolution data (e.g. SPOT-HRV, 20 m spatial resolution) are fine enough to describe the length scales of the landscape (De Cola, 1989; Henebry, 1993; Walsh et al., 1997). Since this study focuses on the description of the spatial heterogeneity at the landscape level, the length scales smaller than the size of the high spatial resolution pixel are thus neglected.

This work aims at using variogram models of high spatial resolution NDVI images (i) to describe the spatial heterogeneity of vegetation cover at the landscape level, (ii) to quantify this spatial heterogeneity at moderate spatial resolution and (iii) to propose an approach for defining a "sufficient pixel size" to capture the spatial variability of the landscape vegetation cover. In Section 2, some image spatial analysis tools are reviewed to underline the potential of the variogram to model the spatial heterogeneity characteristics of the landscape. The 18 contrasted landscapes extracted from the VALERI database and used in this study, are described in Section 3. Section 4 is dedicated to the variogram methodology used to describe and quantify the spatial heterogeneity. In Section 5, the landscape spatial heterogeneity is analyzed with respect to the land use and the vegetation type. Then, the influence of the image size on the characterization of the spatial heterogeneity by the variogram and the limit of the variogram to describe the local spatial heterogeneity are discussed. Finally, the variogram information is used to estimate a sufficient pixel size to capture the landscape spatial variability.

2. Brief review of tools used to characterize the image spatial heterogeneity

Julesz (1962) underlines that first order statistics are not efficient to depict image spatial variations since they do not account for spatial correlation between data. Second order statistics which describe the spatial relationships between data are more appropriate (Gagalowicz, 1983; Haralick & Shanmugan, 1974; Julesz, 1962). Table 1 shows a comparison of the main characteristics of some second order statistics tools used to explore the spatial heterogeneity of an image:

Table 1
Comparison of several tools to explore the image spatial variation (SOA: Second Order Stationary, NA: not applicable)

Tools	Approaches	Hypothesis	Image properties	Data regularization	References
Local variance	Empirical	SOA (implicit)	– Image variance – Length scales	Multiscale formalism	Woodcock and Strahler (1987), Rahman et al. (2003)
Quadtree, hierarchical decomposition	Empirical	SOA (implicit)	– Image variance – Length scales	Multiscale formalism	Woodcock and Harward (1992), Csillag (1997)
Haralick indices	Empirical	SOA (implicit)	– Image variance – Length scales – Correlation	NA	Haralick and Shanmugan (1974), Carr (1996)
Spatial entropy	Probabilistic	SOA	– Spatial disorder	NA	Journel and Deutsch (1993)
Variogram	Probabilistic	SOA or intrinsic	– Image variance – Length scales – Image rugosity (with behavior of the variogram at the origin)	Change of support theorem	Curran (1988), Jupp et al. (1988a), Woodcock et al. (1988a), Lacaze et al. (1994), Chilès and Delfiner (1999), Atkinson (2001)
Fractal	Probabilistic	Intrinsic	– Image rugosity	Power law with only one scale factor	Mandelbrot (1983), De Cola (1989), Lam and De Cola (1993)
Multifractal	Probabilistic	Intrinsic	– Multifractal spectrum	Power law with infinite scale factors	De Cola (1993), Hu et al. (1998), Lovejoy et al. (2001)
Fourier transform	Mathematical or probabilistic	SOA (implicit)	– Image variance – Length scale	NA	Mallat (1999), Cosh and Brutsaert (2003)
Wavelet transform	Mathematical	NA	– Local spatial variation – Local length scale	Multiscale formalism	Hu et al. (1998), Mallat (1999), Csillag and Kabos (2002)

- *Approaches*: Image spatial heterogeneity can be described by using empirical approaches such as Haralick indices, ANOVA-quadtree analysis or local variance. Its characterization by these tools may be limited because of the lack of an underlying theoretical framework. Probabilistic approaches which consider the image as a realization of a stochastic process called random function (Chilès & Delfiner, 1999), provide more efficient tools to model the spatial heterogeneity components. Other methods involve mathematical models such as Fourier transforms or wavelet analysis (Mallat, 1999).
- *Underlying hypothesis*: The characterization of spatial heterogeneity components may involve explicit or implicit hypothesis of stationarity. Stationarity means that the characteristics of the underlying random function are invariant to the shifting of a group of pixels from one part of the image to another (Wackernagel, 2003). Two stationarity hypotheses are commonly used. Second order stationarity supposes the existence and the stationarity of the first two moments of the random function. Intrinsic stationarity assumes second order stationarity of differences between values at two different locations.
- *Image properties*: The variance and the length scales are the main image properties retrieved from second order statistics tools. The characterization of finite length scale requires a second order stationarity assumption. It is achieved by the decomposition of image variance which is either implicit with the variogram (Chilès & Delfiner, 1999; Lacaze et al., 1994; Tian et al., 2002) or explicit with a multiscale representation of the image (Csillag, 1997; Csillag & Kabos, 1996). Note that wavelet analysis is the only method able to detect and quantify properly local spatial variations in the image (Mallat, 1999) since all other methods rely on some stationarity hypothesis.
- *Description of data regularization*: This concept refers to the loss of image spatial variability by aggregating the image at coarser spatial resolution. The variogram tool is specially helpful here since it is able to quantify data regularization through the theory of change of support (Atkinson, 2001; Collins & Woodcock, 1999; Jupp et al., 1988a,b).

The choice of a method depends on the nature of the data, the observational scale and the goals of the study. The NDVI variogram defined in the framework of second order stationarity hypothesis is an appropriate tool to model the characteristics of the spatial heterogeneity of the landscape vegetation cover (spatial variability and length scales). It provides a pertinent understanding of the nature and causes of the image spatial variation (Ramstein & Raffy, 1989; Woodcock et al., 1988a,b) such as the radiometric contrast between the image objects (Bruniquel-Pinel & Gastellu-Etchegorry, 1998; Curran, 1988; St-Onge & Cavayas, 1995; Woodcock et al., 1988a,b), the mean size of the image objects (Lacaze et al., 1994; Woodcock et al., 1988a,b) or the multiscale spatial structuring of the landscape (Lacaze et al., 1994; Oliver, 2001). However, most of these papers are limited to experimental variograms. In this paper, we propose

to retrieve spatial heterogeneity characteristics from variogram models fitted to experimental variograms. We also introduce the concept of integral range, a characteristic derived from variogram models that will be shown to be related to the spatial extent of the image spatial structures. Application of these tools and concepts to a library of 18 images will prove to be powerful for describing and understanding the spatial heterogeneity at the landscape level. Moreover, the modeling of the variogram allows quantifying explicitly the loss of spatial variability as the spatial resolution decreases. This result can then be used to correct the bias induced by spatial heterogeneity when scaling non-linear model at moderate spatial resolution (Garrigues et al., in press).

3. Data description

The data used here are part of the VALERI database (Baret et al., in press), which provides SPOT-HRV scenes at 20 m spatial resolution for several landscapes sampled through the world. For this study, 18 contrasted spatial heterogeneity sites were selected (Table 2). Each site has the following characteristics: 3000 by 3000 m size; flat topography; it contains one or two types of vegetation. The reflectance was measured in four spectral bands: GREEN (0.5–0.59 μm), RED (0.61–0.67 μm), NIR (0.78–0.89 μm) and SWIR (1.58–1.75 μm). Although a fully multivariate analysis is possible (Garrigues, 2004), for the clarity of exposition we limit the analysis of vegetation cover to a univariate measure represented by NDVI (Eq. (1)) computed from RED and NIR reflectances.

$$\mathrm{NDVI} = \frac{\mathrm{NIR}-\mathrm{RED}}{\mathrm{NIR}+\mathrm{RED}}. \quad (1)$$

The SPOT-HRV images are not contaminated by clouds except on the tropical forest image for which a cloud mask was applied. They are not corrected for atmospheric scattering and absorption. But, for most scenes, the atmospheric effects are low in the RED and NIR bands (Baret et al., in press).

4. Methodology

The characterization of landscape spatial heterogeneity from the selected NDVI images requires several hypotheses. H_1: the image extent (3000 m) is large with respect to the spatial features of interest, and any spatial structures extending beyond the image extent is considered as apparent trends. H_2: the radiometric measurement errors (cloud detection, atmospheric effects, resampling effects...) are small relative to the surface variations. Because the combination of the PSF and the sampling step of the sensor are such that effects of spatial variations within a pixel are very small relative to the environmental variations, we state the following third hypothesis. H_3: spatial variations at a scale smaller than the sampling step can be neglected. In addition, we consider high spatial resolution radiometric data as punctual (H_4).

Table 2
Data base (detailed information on each site are available on the VALERI web site www.avignon.inra.fr/valeri)

Site name	Biome (FAO classification)	Date	Latitude	Longitude	m_{NDVI}	σ_{NDVI}
Fundulea01	Cropland	May	44.41	26.58	0.51	0.23
Alpilles01	Cropland	Mar	43.81	4.74	0.41	0.19
Barrax03	Cropland	Jul	39.06	2.10	0.29	0.19
SudOuest02	Cropland	Jul	43.51	1.24	0.50	0.17
Alpilles02	Cropland	Jul	43.81	4.74	0.38	0.16
Gilching02	Cropland and mixed forest	Jul	48.08	11.33	0.60	0.12
Laprida01	Grassland	Nov	36.99	− 60.55	0.62	0.09
Larzac01	Grassland	Jul	43.95	3.12	0.49	0.06
Larose03	Mixed forest	Aug	45.38	−75.22	0.70	0.06
Jarvselja01	Mixed forest	Jul	58.29	27.29	0.82	0.05
Hirsikangas03	Needleleaf forest	Aug	62.64	27.01	0.59	0.09
Nezer01	Needleleaf forest (pine forest)	Jun	44.51	−1.04	0.66	0.06
Concepcion03	Needleleaf forest (80% of pine)	Jan	−37.47	−73.47	0.69	0.09
Aekloba01	Broadleaf forest (Palmtree plantation)	Jun	2.63	99.68	0.65	0.04
Counami01	Broadleaf forest (tropical forest)	Oct	05.35	53.25	0.69	0.03
Puechabon01	Closed shrubland (Med. vegetation)	Jun	43.72	3.65	0.54	0.10
Gourma00	Savanna	Sep	15.32	−1.55	0.22	0.01
Turco02	Barren and sparse vegetation	Aug	−18.23	−68.18	0.11	0.01

Date is the acquisition month of the image. m_{NDVI} and σ_{NDVI} are the mean and standard deviation of the NDVI image.

The approach follows two steps. The experimental variogram is first computed at the image scale. A probabilistic framework is then used to model the spatial heterogeneity components through the experimental variogram.

4.1. Experimental variogram

NDVI data are considered as values of a punctual regionalized variable $z(x)$, i.e. a numeric function of geographic location (Matheron, 1965), which describes the spatial distribution of the landscape vegetation cover over the image domain, I. The experimental variogram measures the average of squared differences between values $z(x_\alpha)$ and $z(x_\beta)$ of paired pixels (x_α, x_β) separated by a vector $\boldsymbol{h}$ (Eq. (2)).

$$\gamma_e(\boldsymbol{h}) = \frac{1}{2N(\boldsymbol{h})} \sum_{||x_\alpha - x_\beta|| \approx \boldsymbol{h}} (z(x_\alpha) - z(x_\beta))^2. \quad (2)$$

Experimental variograms can be computed for a specific direction ($\boldsymbol{h}$ is then a vector in Eq. (2)) or without specifying a direction ($\boldsymbol{h}$ is reduced to a distance in Eq. (2)). Variogram values are not statistically reliable at large distances (Chilès & Delfiner, 1999). We therefore decided to compute the variogram up to the maximum distance $d_{max}=1500$ m equal to half the extent of the images, as advised by these authors. An experimental variogram is characterized by several key properties (Chilès & Delfiner, 1999). It is usually an increasing function of the distance $||\boldsymbol{h}||$ (Fig. 1) since values of pixels close together are likely to be more similar than values of far apart pixels. At large distance, it may reach a sill or increase indefinitely. Most of the variograms computed on the images of the VALERI database reach a sill before d_{max}. The sill is an indicator of the spatial variability of the data. The range is the distance at which the variogram reaches the sill. If the sill is not reached before d_{max}, the spatial variability is not completely encompassed at the image scale. The behavior of the variogram near the origin is an important property of the variogram which reflects the continuity of the variable under study. In particular, a discontinuity of the variogram at the origin, also called nugget effect, can be related to either uncorrelated noise (measurement error) or to spatial structures at a length scale smaller than the pixel size. All experimental variograms computed on the VALERI images are linear at the origin, without any nugget effect. This observation is a strong support to the hypotheses (H_2) and (H_3). In this work, the spatial distribution of NDVI is assumed to be isotropic and the experimental variograms are computed by pooling together all directions. This assumption is not absolutely necessary. However, since isotropy is verified for most of the 18 images analyzed in this paper, we introduce it for the clarity of exposition. The methodology presented below can easily be extended to the case of non-isotropic variogram models.

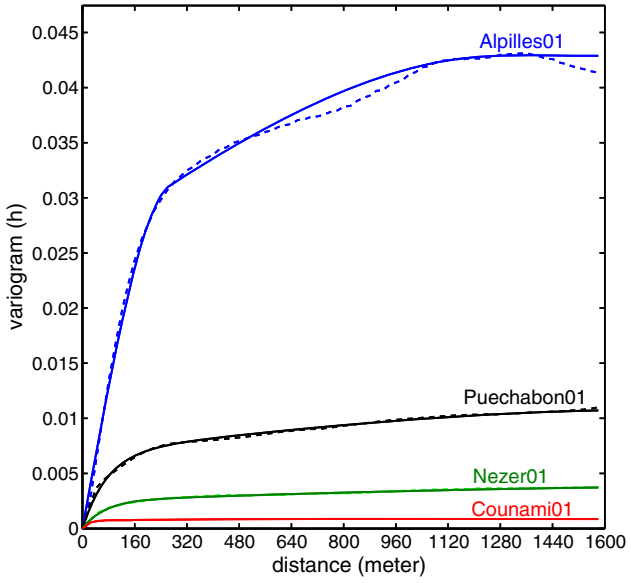

Fig. 1. NDVI variograms of four contrasted landscapes. The dash lines are the experimental variograms. The solid lines represent the fitted variogram models. The parameters of the variogram models are given in Table 4.

4.2. Variogram modeling

The experimental variogram provides an empirical description of the NDVI spatial distribution using second order statistics. A probabilistic model for the regionalized variable $z(x)$ is used to provide a parametric characterization of spatial heterogeneity components. $z(x)$ is regarded as one among all possible realizations of the random function $Z(x)$ (Chilès & Delfiner, 1999; Wackernagel, 2003). Second order stationarity of $Z(x)$ assumes the existence and the stationarity of its first and second moments,

$$E[Z(x)] = m \qquad \mathrm{Cov}(Z(x), Z(x+\boldsymbol{h})) = C(\boldsymbol{h}), \quad (3)$$

for all x and $\boldsymbol{h}$. The function $C(\boldsymbol{h})$ is the covariance function of $Z(x)$; it characterizes the spatial distribution of $Z(x)$. Under second order stationarity assumption, the theoretical variogram,

$$\gamma(\boldsymbol{h}) = 0.5\mathrm{Var}[Z(x+\boldsymbol{h}) - Z(x)], \quad (4)$$

is related to the covariance function according to the relationship,

$$\gamma(\boldsymbol{h}) = \sigma^2 - C(\boldsymbol{h}), \quad (5)$$

where σ^2 is the variance of $Z(x)$. The theoretical variogram is a function starting from 0 for $||\boldsymbol{h}||=0$ and ultimately converging to the sill σ^2 as $||\boldsymbol{h}||$ tends to infinity. The range of the theoretical variogram is the distance at which it reaches a sill. Data separated by a distance larger than the range are uncorrelated.

The theoretical variogram is estimated by fitting a valid mathematical function to the experimental variogram (Chilès & Delfiner, 1999). These functions, also called authorized models, must be conditionally negative functions (Wackernagel, 2003). Exponential and spherical models are used in this work since they suit the main properties of the experimental variograms: linear behavior and continuity at the origin; convergence to a sill. Fig. 2a and Table 3 illustrate these two elementary models and their main characteristics. Note that the range parameter of the exponential model is the so called practical range, i.e. the distance at which the variogram reaches 95% of the sill.

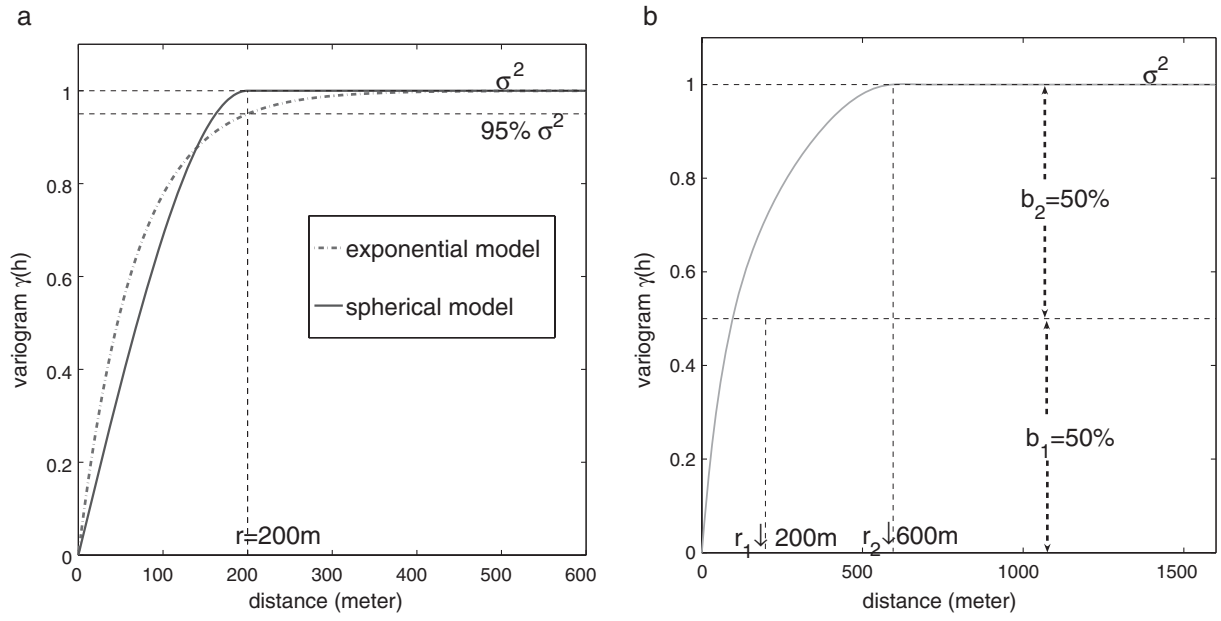

Fig. 2. Theoretical models of the variogram a/: exponential and spherical elementary models with a range r equal to 200 m. b/: linear model of regionalization: sum of an exponential (r_1=200 m, b_1=50%) and a spherical model (r_2=600 m, b_2=50%).

To account for the multiple length scales of the data, a linear combination of the above functions is used to model the variogram. This extended model of variogram (Eq. (6)), called linear model of regionalization (Wackernagel, 2003), is a weighted sum of l elementary variogram models, $g_k(r_k,\boldsymbol{h})$, $k=1,\ldots, l$:

$$\gamma(\boldsymbol{h}) = \sigma^2 \sum_{k=1}^{k=l} b_k g_k(r_k, \boldsymbol{h}). \quad (6)$$

This model is particularly appropriate to describe independent sets of spatial structures, related to different length scales and spatial variability, being overlaid in the same region. It describes both components of spatial heterogeneity as defined in the Introduction (Fig. 2b):

- the degree of image spatial variability is given by the sill σ^2
- the image spatial structures are characterized by the parameters corresponding to each elementary model g_k: range r_k and fraction of the total variance b_k related to each range r_k.

Table 3
Characteristics of the spherical and exponential variogram models

Model	Formula ($\gamma(\boldsymbol{h})$)	Integral range (A)
Spherical	$\gamma(\boldsymbol{h}) = \begin{cases} \sigma^2\left(\frac{3}{2}\frac{\boldsymbol{h}}{r} - \frac{1}{2}\left(\frac{\boldsymbol{h}}{r}\right)^3\right) & \text{if } \boldsymbol{h}\le r \\ \sigma^2 & \text{if } \boldsymbol{h}>r \end{cases}$	$\frac{\pi r^2}{5}$
Exponential	$\gamma(\boldsymbol{h}) = \sigma^2\left(1-\exp\left(-\frac{3\boldsymbol{h}}{r}\right)\right)$	$\frac{2\pi r^2}{9}$

The parameters of $\gamma(\boldsymbol{h})$ are estimated by a semi-automatic fitting method (Isatis software, http://www.geovariances.com). The number of necessary elementary variograms, l, and the associated ranges are visually adjusted. Here, it is always found sufficient to have l equal to one or two. Then, the sill and the variance weights are estimated by weighted mean square optimization, as described by Cressie (1985). Since experimental variograms are not trustworthy for distances larger than $d_{\max}$, any estimated variogram range above this distance is deemed not reliable and therefore was not considered. In this case, the underlying second order stationarity hypothesis must be rejected.

4.3. Characterization of the image spatial structures

The structural information of the variogram provided by the ranges r_k and the fraction of total variance b_k is summarized in a single parameter: the integral range (A). The integral range of a second order stationary random function $Z(x)$ is defined by Eq. (7) (Chilès & Delfiner, 1999; Lantuéjoul, 2002) :

$$A = \frac{1}{\sigma^2}\int_{\boldsymbol{h}\in\Re^2} (\sigma^2 - \gamma(\boldsymbol{h}))\mathrm{d}\boldsymbol{h}. \quad (7)$$

Table 3 gives the value of A for the spherical and exponential models (Lantuéjoul, 2002). For a linear model of regionalization, A is a weighted linear combination of the integral range of each elementary model, A_k:

$$A = \sum_{k=1}^{l} b_k A_k, \qquad A_k = \int_{\boldsymbol{h}\in\Re^2} (1 - g_k(r_k, \boldsymbol{h}))\mathrm{d}\boldsymbol{h} \quad (8)$$

The integral range is an area moment (Serra, 1982). The ergodic covariance theorem (Chilès & Delfiner, 1999; Lantuéjoul, 2002) states that if the image domain, I, is large with

respect to the integral range, the variance of the spatial average of $Z(x)$ over I, denoted $\overline{Z}_I$, is

$$\mathrm{Var}(\overline{Z}_I) \approx \frac{\sigma^2 A}{|I|} \tag{9}$$

Hence, if compared with the conventional formula for the variance of an arithmetic average of M independent points, the ratio $M=|I|/A$ can be seen as the equivalent number of independent values in I. The integral range A can be considered as their equivalent area of influence. Its square root, denoted D_c, is thus the distance between those M 'independent data', as if they were located on a regular square grid. D_c summarizes all structural parameters of the fitted model into a single characteristic distance which is the weighted average of the different range parameters. We chose to call it the 'mean length scale' of the NDVI image under study. It is related to the mean extent of the image spatial structures. A and D_c may be used as yardsticks to judge if the size of an image is large enough to detect the length scales of the landscape in this image (hypothesis H_1). We state that hypothesis (H_1) is verified if the variance of $\overline{Z}_I$ is negligible, i.e. if the integral range A is smaller than 5% of the image surface $|I|$. Therefore, for a 3 by 3 km image, if A is smaller than the threshold $A_{T,3\ km}=4.5.10^5\ m^2$, i.e. if D_c is smaller than $D_{c,T,3\ km}=671$ m, the image size is considered to be large enough to characterize the image spatial structures by the variogram. Among the 18 images under study, 12 verify the hypothesis H_1.

4.4. Quantification of the spatial heterogeneity

In the previous sections, the variogram was used to describe the spatial distribution of the NDVI at the image scale. It can be also used to quantify the spatial heterogeneity of a sub-domain of the image. In the following, the high spatial resolution image is partitioned into P congruent blocks v_i by shifting a generic block domain (v). The image spatial variability is decomposed at 3 spatial scales (Atkinson, 2001; Chilès & Delfiner, 1999; Myers, 1997)

- The experimental dispersion variance of the N high spatial resolution pixel values within the image (i.e. image variance),

$$s^2(x|I) = \frac{1}{N}\sum_{\alpha=1}^{N} (z(x_\alpha)-\overline{z}_I)^2, \tag{10}$$

where $\overline{z}_I$ is the spatial average of $z(x)$ over the image.

- The experimental dispersion variance of the P block values within the image (i.e. between block variability),

$$s^2(v|I) = \frac{1}{P}\sum_{i=1}^{P} (\overline{z}_{v_i}-\overline{z}_I)^2, \tag{11}$$

where $\overline{z}_{v_i}$ is the spatial average of $z(x)$ over the domain v_i.

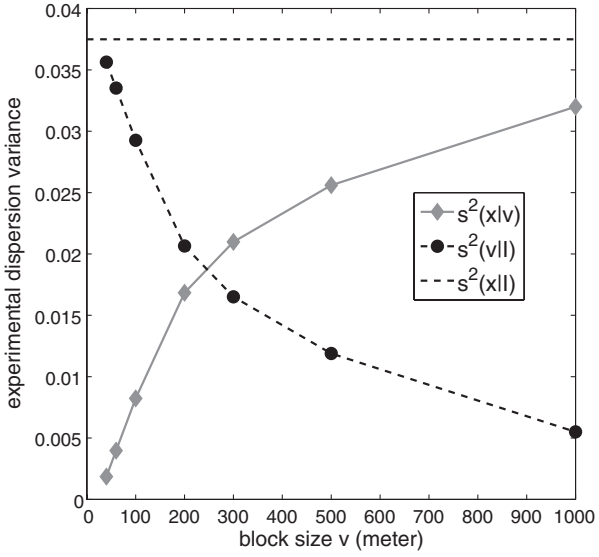

Fig. 3. Intra-block dispersion variance $s^2(x|v)$ and between-block dispersion variance $s^2(v|I)$ as a function of the block size v for an NDVI image (Alpilles01). $s^2(x|I)$ is the variance of the high spatial resolution image.

- The average experimental dispersion variance of the n high resolution pixel values within the blocks (i.e. intra-block variability),

$$s^2(x|v) = \frac{1}{P}\sum_{i=1}^{P} \frac{1}{n}\sum_{\alpha=1}^{n} (z(x_\alpha)-\overline{z}_{v_i})^2. \tag{12}$$

The decomposition of the image spatial variability is summarized by Eq. (13):

$$s^2(x|I) = s^2(v|I) + s^2(x|v). \tag{13}$$

As shown in Fig. 3, as the size of the block v increases, the intra-block variability increases and the between block variability decreases. $s^2(x|v)$ quantifies empirically the loss of image variability when aggregating the pixels to a coarser resolution. It can be computed directly from the theoretical variogram of the high resolution image. In the framework of stationary of order 2 random functions, $s^2(x|v)$ is a realization of a random variable $S^2(x|v)$. The theoretical dispersion variance $\sigma^2(x|v)$ of $Z(x)$ within the domain v is defined as the mathematical expectation of $S^2(x|v)$ (Wackernagel, 2003):

$$\sigma^2(x|v) = E[S^2(x|v)] \tag{14}$$

It can be shown that the theoretical dispersion variance is equal to the double integration of the theoretical variogram over the domain v (Eq. (15), Chilès & Delfiner, 1999),

$$\sigma^2(x|v) = \gamma(v,v) = \frac{1}{|v|^2}\int_{x\in v}\int_{y\in v} \gamma||x-y||\mathrm{d}x\mathrm{d}y, \tag{15}$$

where $||x-y||$ represents the distance between the points x and y of the domain v and $|v|$ the area of v.

$\gamma(v,v)$ quantifies the degree of spatial heterogeneity within a generic sub-domain v of the image. It is computed for several

size of v (60, 100, 200, 300, 500 and 1000 m). As v increases, $\gamma(v,v)$ tends asymptotically towards the sill σ^2. When the sill is reached, data are completely regularized, i.e. the aggregation of the pixels to a coarser resolution does not engender more loss of image variability. We define TH_v, the rate of data regularization, i.e. the rate of the loss of image spatial variability, at a given spatial resolution v.

$$TH_v = \frac{100\gamma(v,v)}{\sigma^2}. \quad (16)$$

Its values at several spatial resolutions characterize how fast $\gamma(v,v)$ converges to the sill.

5. Results

5.1. Variogram analysis of four contrasted landscapes

To show the ability of the variogram to depict landscape spatial heterogeneity, the variograms are first analyzed on four contrasted landscapes (Figs. 1 and 4): cropland (Alpilles01), closed shrubland (Puechabon01), pine forest (Nezer01) and tropical forest (Counami01).

The image spatial variability, σ^2, increases considerably from tropical forest (Counami01) to cropland (Alpilles01). Nezer01 and Counami01 have a low sill because the important development of vegetation and the presence of green understory limit the variability of the landscape vegetation cover. However, because NDVI saturates for dense vegetation, its spatial distribution may not resolve the whole vegetation cover variability of these sites. The high variability of Alpilles01 is explained by the mosaic of vegetation field (winter wheat at the maximum of greenness) with high NDVI values and bare soil field (not developed summer crops) with low NDVI values. The intermediate sill value of Puechabon01 is due to the intrinsic variability of Mediterranean vegetation structure (presence of open areas, variation of the vegetation height and density …), as well as some objects (road, quarry, rocky area…) with low NDVI values contrasting with the vegetation area.

The shape of the variograms provides an understanding of the NDVI spatial structures within the image domain. The variograms of Fig. 1 have been modeled using the linear model of regionalization with two spatial structures. On Counami01 the variogram increases promptly and reaches almost the whole image variance at a very short range (r_1=57 m; b_1=85%). This landscape is thus poorly structured at the observational scale under study. Concerning the three other sites, their variograms show larger spatial structures (r_1 between 200 and 300 m). On Alpilles01, the first spatial structure (r_1=268 m) is related to the mosaic of the agricultural fields, with a value similar to the average extent (250–350 m) of the fields. The associated variance (b_1=60.5%) characterizes the important variability of vegetation cover between fields which is the main cause of the spatial variability of this landscape. On Puechabon01, the first spatial

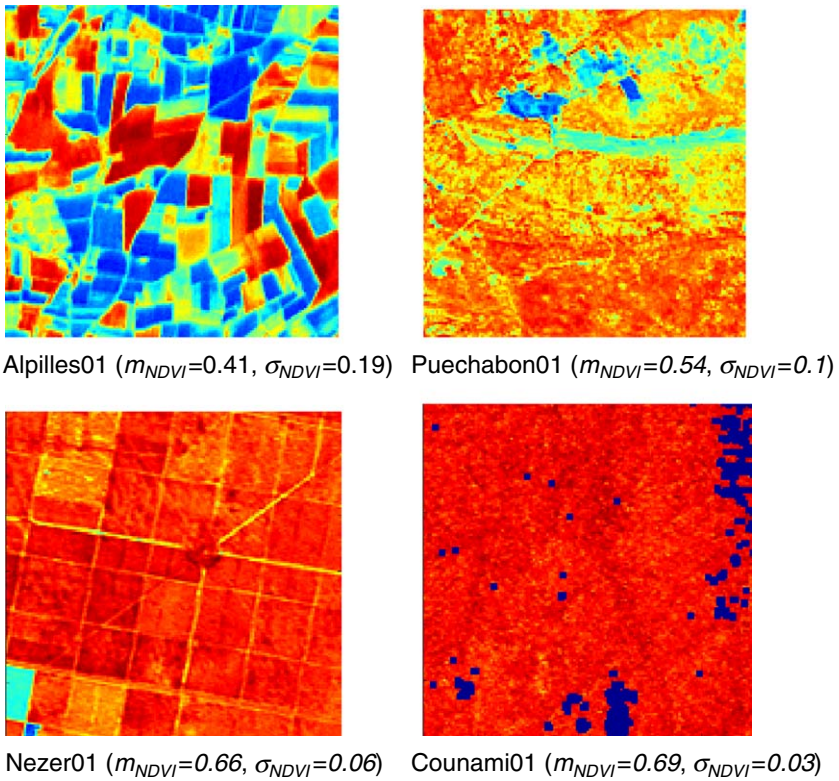

Fig. 4. NDVI images of four contrasted landscapes: Alpilles01: cropland; Puechabon01: closed shrubland — Mediterranean vegetation; Nezer01: pine forest; Counami01: tropical forest. The blue pixels on the Counami01 image represent cloud pixels. These are not taken into account in the calculation of the variogram.

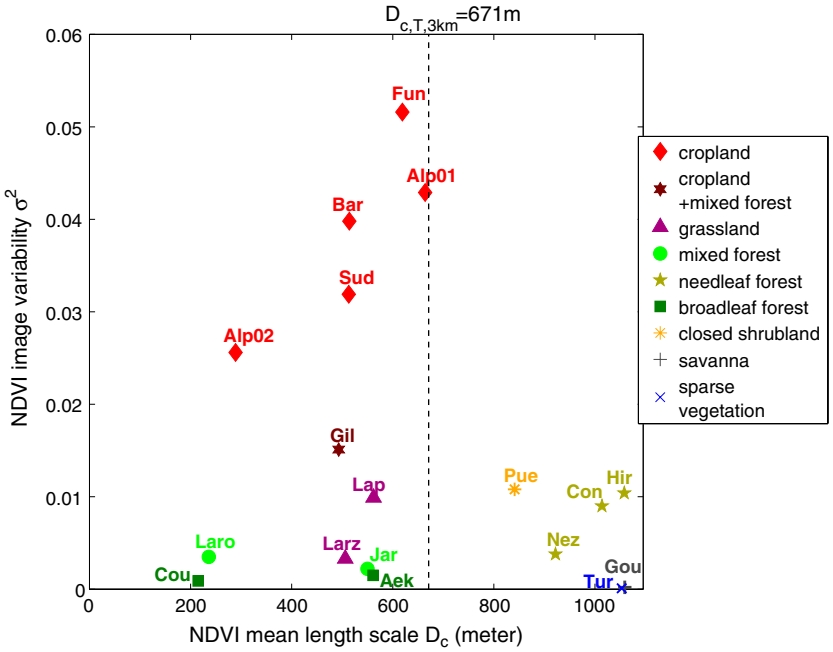

Fig. 5. NDVI spatial variability (σ^2: variogram sill) versus the NDVI mean length scale (D_c: square root of the variogram integral range) for the 18 landscapes under study.

structure (r_1 = 230 m) has a fuzzier shape than that of Alpilles01. It results both from the intrinsic length scale of Mediterranean vegetation and the presence of incongruent objects in the landscape (quarry, roads…). The Nezer01 image has a rectangular field patterns but its first range (r_1 = 205 m) is shorter than the field extent (around 500 m). The field structure is not detected by the variogram because of the limited NDVI variability between fields. The first spatial structure describes the intra-field spatial variability of the understory cover or some spatial variations of the plantation density. The second spatial structure of Alpilles01, Nezer01 and Puechabon01 explains a low part of the landscape spatial variability (less than 40%). On Alpilles01, it may be caused by the soil variability. The variograms of Puechabon01 and Nezer01 do not reach a sill at a distance lower than 1500 m. As a consequence, the characterization of their second range is very uncertain since the whole spatial variability is not encompassed at the image scale. As shown on these four landscapes, the NDVI variogram describes efficiently the spatial heterogeneity of vegetation cover. The analysis is now extended to the 14 other landscapes of the database.

Table 4
Parameters of the fitted variogram models

Site name	σ^2	$g_1(r_1)$; b_1	$g_2(r_2)$; b_2	D_c	TH_{100}	TH_{300}	TH_{500}	TH_{1000}
Fundulea01	0.0516	*Sph* (781)	/	619	10	29	47	76
Alpilles01	0.0429	*Sph* (268); 60.5	*Sph* (1290); 39.5	664	19	50	64	80
Barrax03	0.0398	*Sph* (648)	/	514	12	35	55	82
SudOuest02	0.0319	*Sph* (356); 50.1	*Sph* (844); 49.9	513	15	43	62	83
Alpilles02	0.0256	*Sph* (184); 26.3	*Sph* (410); 73.7	289	24	61	79	93
Gilching02	0.0151	*Exp* (525); 91.6	*Sph* (1125); 8.4	493	23	52	68	86
Laprida01	0.0099	*Exp* (216); 53.8	*Sph* (1014); 46.2	562	29	54	66	83
Larzac01	0.0033	*Exp* (289); 83.4	*Sph* (1410); 16.6	506	33	64	77	88
Larose03	0.0035	*Exp* (200); 88.3	*Sph* (650); 11.7	236	46	78	88	96
Jarvselja01	0.0022	*Exp* (234); 81.3	*Sph* (1515); 18.7	550	38	68	78	88
Hirsikangas03	0.0104	*Exp* (200); 56.0	*Sph* (2000); 44.0	1058	30	44	60	71
Nezer01	0.0038	*Exp* (205); 66.9	*Sph* (2000); 33.1	922	34	59	68	78
Concepcion03	0.0090	*Exp* (150); 19.4	*Exp* (1350); 80.6	1014	20	40	52	71
Aekloba01	0.0015	*Exp* (150); 85.2	*Sph* (1800); 14.8	561	51	78	84	90
Counami01	0.0009	*Exp* (57); 85.0	*Sph*(687); 15.0	215	74	88	92	97
Puechabon01	0.0108	*Exp* (230); 64.4	*Sph* (1750); 35.6	841	31	56	66	78
Gourma00	0.0002	*Exp* (67); 55.4	*Sph* (2000); 44.6	1059	47	59	64	72
Turco02	0.0001	*Exp* (300); 57.3	*Sph* (2000); 42.7	1053	23	46	57	70

σ^2 is the sill (image spatial variability); g_1 and g_2 are the elementary variogram models; *Exp*: exponential model; *Sph*: spherical model; r_1 and r_2: variogram ranges, in meter; b_1 and b_2: fraction of total variance, in %; D_c: square root of the integral range, in meter; TH_v : rate of the loss of NDVI spatial variability (in %) at the spatial resolution *v*.

5.2. Description of the spatial heterogeneity at the landscape level

In order to understand the main factors influencing spatial heterogeneity at the landscape level, we now compare the spatial heterogeneity characteristics σ^2 and D_c of the 18 landscapes (Fig. 5, Table 4).

5.2.1. Spatial variability

The differences of NDVI spatial variability between landscapes (σ^2 is between 0.0001 and 0.052) are mainly explained by the type of landscape. Crop sites are the most heterogeneous ($\sigma^2 > 0.02$). Their spatial variability is explained by the differences of NDVI values between fields caused by the nature and state of the crop. The mosaic of bare soil fields with low NDVI and crop fields with high NDVI, as is the case when the site contains both winter and summer crops, increases dramatically the NDVI spatial variability. Natural vegetation and forest sites are more homogeneous than crop sites at the landscape level (for most of these sites $\sigma^2 < 0.008$). The important vegetation cover of the forests (NDVI around 0.7) which includes the green understory, the high density of trees, or the presence of broadleaves, homogenizes the distribution of NDVI values. Medium vegetation cover sites with NDVI around 0.49 (grassland) and low vegetation cover sites with NDVI around 0.17 (savanna and shrubland) are homogeneous at the landscape level. However, the type of landscape is not always sufficient to explain the landscape spatial variability. Indeed, on some sites, the atypical sill ($0.008 < \sigma^2 < 0.02$) with regard to their vegetation type is explained by additional factors. First, the heterogeneity of land use within the observed area may increase or decrease the spatial variability. For example, on Concepcion03 and Hirsikangas03, the contrast between low NDVI areas (young seedling plantation, bare soil and water area) and high NDVI values of the forest, increases the spatial variability of these landscapes. Conversely, on Gilching02 the presence of a homogeneous forest area explains that the sill value is lower than the other crop sites. Second, other environmental factors such as the presence of water (Laprida01, Larose03) or the variation of soil properties (soil salinity on Laprida01) may also be sources of NDVI spatial variability.

5.2.2. Mean length scale

The mean extent of the image spatial structures, quantified by the mean length scale D_c, does not show a strong dependency with respect to the type of landscape. On the 18 sites under study, it varies from 215 to 1059 m. For the clarity of exposition, the spatial structures are analyzed per type of landscape, as follows.

On crop sites, D_c varies from 289 to 664 m. Their length scales are completely characterized at the image scale ($D_c < D_{c,T,3\ km}$). NDVI discontinuities between fields create a mosaic spatial structure resulting mainly from anthropogenic processes (field size, seedling and harvesting date, crop rotation…). The extent of the cropland spatial structures is mainly influenced by the size of the fields. It varies from large fields (Fundulea01, $D_c = 619$ m; Barrax02, $D_c = 514$ m) to small fields (Alpilles02, $D_c = 289$ m). However, the characterization of the field sizes by the variogram ranges is a non-trivial issue. Indeed, it may be disturbed by the gathering of fields with similar NDVI values which create larger spatial structures (e.g. the second range of SudOuest02). Consequently, NDVI spatial structures are not only intrinsic properties of the landscape but depend also on the season. For example, on the Barrax03 NDVI image acquired in July, irrigation discs of vegetation are laid over a large bare soil background. Since NDVI describes the vegetation cover, its variogram detects only the disc spatial structures and not the spatial structures within the bare soil area. The result would be different with other acquisition dates. Besides, a radiometric variable more sensitive to soil properties than NDVI (like RED reflectance) may capture better the spatial structures within the bare soil area.

On natural vegetation and forest sites, D_c varies from 215 to 1059 m. Their spatial structures have a fuzzier pattern associated with smoother NDVI discontinuities than crop field structures. They are caused by several factors such as ecological processes (light availability, species competition), environmental processes (presence of water, soil salinity), geomorphologic factors (micro-relief, rocky area), seasons (variation of the understory cover) and human factors (forest exploitation, grazing intensity on grassland).

Gilching02 is composed of a forest area and a crop area. Its variogram is particularly interesting since it provides a characterization of both forest and crop spatial structures. The first range ($r_1 = 525$ m) which explains 92% of the image variance may be explained by the field structure of the crop area. The larger range ($r_2 = 1150$ m) is probably related to the fuzzier spatial structure within the forest area which is less variable at the image scale. This example underlines that the field spatial structure of cropland is the main source of NDVI variability at the landscape level.

In opposition to crop sites, the length scales of natural and forest sites are not always completely characterized at the image scale. Indeed, NDVI images with $D_c > D_{c,T,3\ km}$ are not large enough to encompass the whole landscape variability. It is caused by the presence of a large spatial structure with respect to the size of the image, related to an important part of the image variability. For some of these sites the second range is higher than d_{max}. As mentioned before, the underlying second order stationarity hypothesis is rejected for these sites. On Puechabon01, the presence of a contrasted spatial structure in the border of the image may be the cause of lack of stationary sill at the image scale.

This analysis provides some understanding of the spatial heterogeneity factors at the landscape level. The variogram sill (σ^2) is an indicator of the landscape variability. The main factor of spatial heterogeneity at the landscape level is the variability of the land use which is mostly influenced by anthropogenic processes. Croplands are the most heterogeneous sites. Their field spatial structure is an important source of landscape spatial variability. Natural vegetation and forest sites are more homogeneous at the landscape level. Typical length scales of the landscapes studied in this work, as measured by D_c, vary from 215 to 1059 m. This information will be used in the Discussion section to define a sufficient spatial resolution at which the major part of the landscape spatial variability is captured by the sensor.

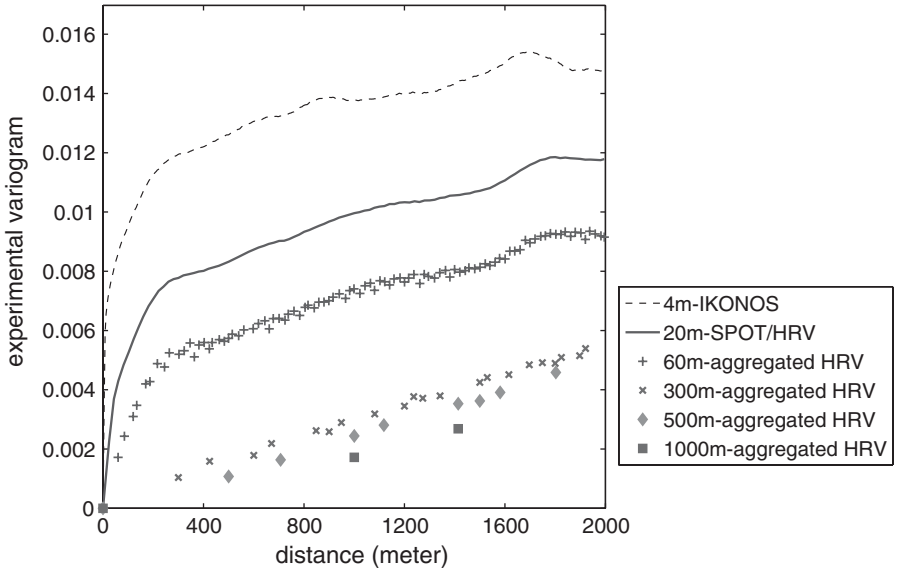

Fig. 6. Effect of decreasing the image spatial resolution on the NDVI variogram (Puechabon01 site). Each line corresponds either to a different sensor (IKONOS or SPOT-HRV) or to the 20 m SPOT-HRV aggregated at coarser spatial resolution (60, 300, 500 or 1000 m).

5.3. Spatial heterogeneity as a function of spatial resolution

Fig. 6 shows the variograms of several NDVI images of the same site (Puechabon01) originating from Ikonos (4 m) and SPOT-HRV (20 m) sensors with close acquisition dates or from the aggregation of SPOT-HRV 20 m NDVI image at coarser spatial resolution (60, 300, 500, 1000 m). The variogram changes with the spatial resolution describe the effect of data regularization on the spatial heterogeneity components. The fall of the sill characterizes the loss of spatial variability when the spatial resolution decreases. NDVI variability discrepancy between Ikonos and SPOT-HRV underlines the different landscape features detected by these two sensors. There are more pure vegetation or rocky pixels on the Ikonos image, thus increasing the NDVI variability. Other factors such as the PSF of each instrument or the differences in the atmospheric conditions between the acquisition dates may explain the difference of the sill value between the two images.

Moreover, the variograms get more regular as the spatial resolution decreases. At 4, 20 and 60 m resolutions variograms have similar shape and detect the same length scales. But, for spatial resolution coarser than 300 m, the first length scale at 230 m is not detected by the variogram. As a consequence, a spatial structure cannot be resolved by the sensor when the pixel size is larger than its length scale.

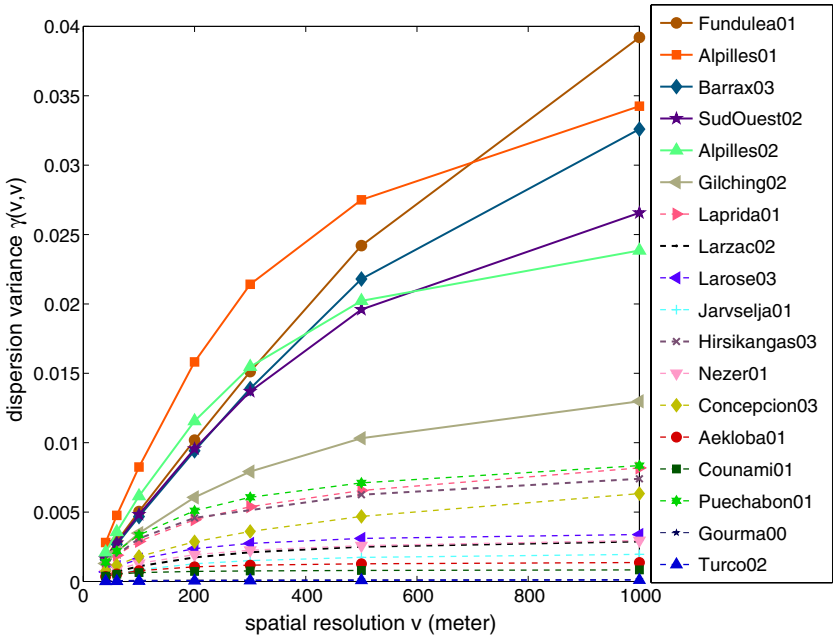

Fig. 7. Theoretical dispersion variance $\gamma(v,v)$ as a function of the spatial resolution v. The solid lines are cropland sites and the dash lines are natural vegetation and forest sites.

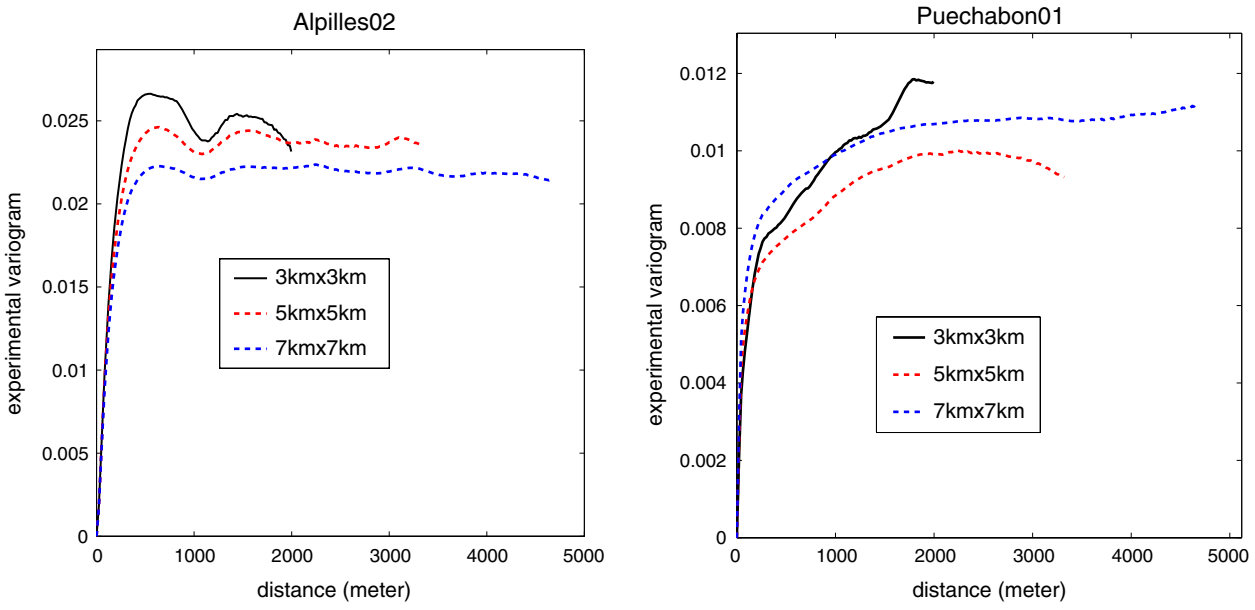

Fig. 8. Effect of image size on the experimental variogram on Alpilles02 and Puechabon01.

An important issue emerging from this work is how to quantify the loss of spatial heterogeneity at coarser resolution. As mentioned in Section 4.4, the dispersion variance $\gamma(v,v)$ represents the spatial heterogeneity degree within the coarse resolution pixel. As shown on Fig. 7, the rate at which the dispersion variance increases with the pixel size is explained by the heterogeneity characteristics of the landscape displayed in Fig. 5. For example, on the weakly structured site Counami01 (D_c=215 m), NDVI data are almost completely regularized at 300 m spatial resolution (Table 4: TH_{300}=88%, TH_{1000}=97%). But on Alpilles01 the regularization is less important (Table 4: TH_{300}=49%, TH_{1000}=82%) because of the presence of a spatial structure at a larger length scale (D_c=664 m). At a given spatial resolution, the dispersion variance $\gamma(v,v)$ depends on σ^2 and on the ratio between the image length scale and the pixel size. For example, at 500 m spatial resolution, the dispersion variance of Alpilles01 is higher than that of Fundulea01 although its variance σ^2 is lower (Fig. 7). At this spatial resolution, since the Fundulea01 length scale (781 m) is still detected by the sensor (TH_{500}=47%), the heterogeneity of the 500 m coarse pixel is low. However, on Alpilles01 since the important spatial variability (b_1=61%) related to the first length scale (r_1=268 m) is lost at 500 m spatial

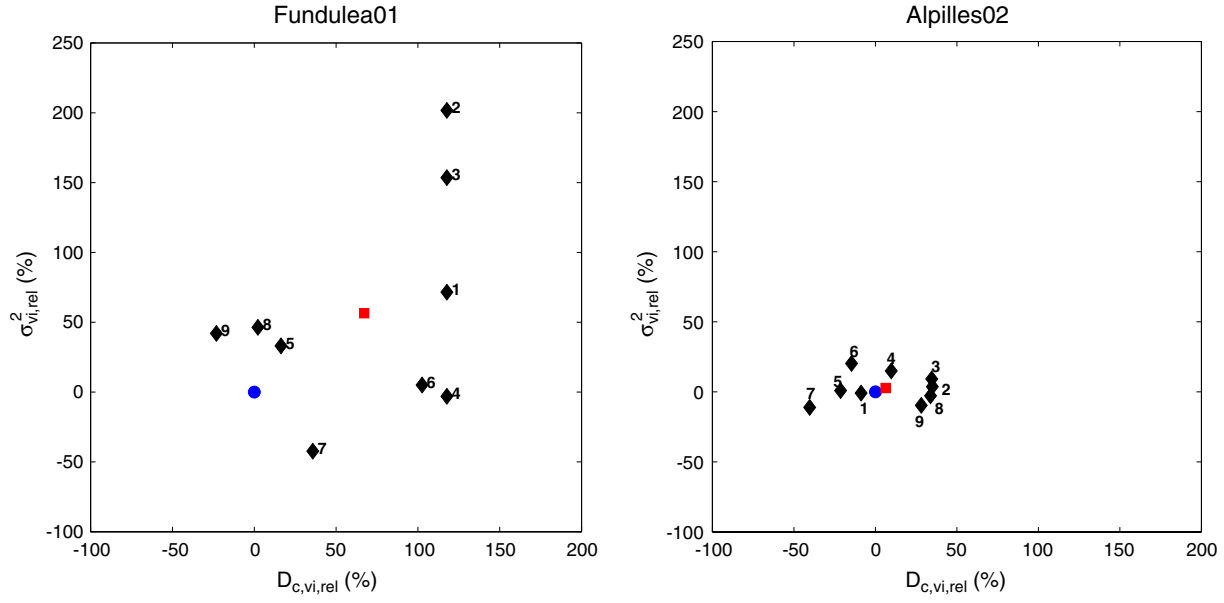

Fig. 9. Local spatial heterogeneity characteristics (D_{c,v_i} and $\sigma_{v_i}^2$) of the 1000 × 1000 m sub-domains v_i (i=1,…, 9) of the partitioned image relative to those computed at the image scale (D_c and σ^2). Each black diamond represents a sub-domain v_i of the partitioned image. The blue circle locates the origin corresponding to the characteristics σ^2 and D_c of the image. The red square represents the mean of $D_{c,v_i,\,rel}$ and $\sigma^2_{v_i,\,rel}$.

resolution (TH_{500}=64%), the dispersion variance of the 500 m coarse pixel is high. At 1000 m spatial resolution, Fundulea01 length scale is not detected any more by the sensor. Hence, since its image variability σ^2 is higher than Alpilles01, Fundulea01 $\gamma(v,v)$ is higher.

The variogram is an efficient tool to quantify the regularization of the data at moderate spatial resolution. The intra-pixel spatial heterogeneity, quantified by the dispersion variance $\gamma(v,v)$, increases rapidly with pixel size until this size is larger than the mean length scale of the data. It then tends asymptotically to the sill of the variogram σ^2. Generally speaking, at 1000 m spatial resolution, the difference of dispersion variance between the sites under study is fully explained by the image variability σ^2.

6. Discussion

The characterization of spatial heterogeneity addresses several issues which are discussed here.

6.1. Effect of image extent on the characterization of spatial heterogeneity

We proposed a criterion to assess if a 3000 m image is large enough to characterize and quantify its spatial heterogeneity: the mean length scale, D_c, must be smaller than the threshold $D_{c,T,3\ km}$=671 m. The presence of a stationary sill on the experimental variogram is a necessary condition, but it is not a sufficient condition. The previous analysis shows that on some landscapes, because of the presence of a large spatial structure with respect to the size of the image, the NDVI spatial variability is not completely encompassed at the image scale.

Fig. 8 illustrates the effect of increasing the image size on the experimental variogram. On Alpilles02, for which D_c=289 m is smaller than $D_{c,T,3\ km}$, the variogram shape does not change when the size of the image increases. On Puechabon01, the experimental variogram of the 3000×3000 m image does not reach its sill before d_{max}=1500 m: r_2=1750 m and D_c=841 m, which is larger than $D_{c,T,3\ km}$. But the experimental variogram computed over the 7000×7000 m image centered on the same location reaches a sill. On this site and on some others, increasing the image size leads to a better characterization of the landscape length scales. However, this may not be true for all sites, because new spatial structures may appear on a larger scene. If their extent is too large with respect to the new image size, they cannot be completely described by the variogram.

The characterization of the spatial heterogeneity is therefore strongly dependent on the observational scale. The D_c criterion can be used to check a posteriori if the image size is large enough to quantify properly the landscape length scales by the variogram. Note that it is the case for most of the sites studied in this work, and especially for all the heterogeneous cropland sites.

6.2. Characterization of the local spatial heterogeneity by the variogram

The spatial variability (σ^2) and the mean length scale (D_c) represent spatial averages of the spatial heterogeneity characteristics at the image scale. To test if they are representative at the local scale, they are modeled on the nine 1000×1000 m sub-domains of the partitioned image. The local spatial heterogeneity characteristics are investigated on Alpilles02 (small fields) and Fundulea01 (large fields). Fig. 9 displays for each sub-domain v_i, i=1,…,9, the value of the local mean length scale D_{c,v_i} relative to the image mean length scale D_c,

$$D_{c,v_i,\mathrm{rel}} = 100\frac{D_{c,v_i}-D_c}{D_c}, \tag{17}$$

and the value of the local sill σ^2_{vi} relative to the image sill σ^2,

$$\sigma^2_{v_i,\mathrm{rel}} = 100\frac{\sigma^2_{v_i}-\sigma^2}{\sigma^2}. \tag{18}$$

On Fundulea01 the extent of the field spatial structure and the size of the 1000 m sub-domains are close. As a consequence, there is an important variability of the characteristics computed on the nine sub-domains and a large difference between their average and the characteristics computed at the full image scale (Fig. 9). On the contrary, on Alpilles02, the image variogram characterizes well the local characteristics of the spatial heterogeneity. The first range (184 m) describes the small fields such as those of the sub-domain v_7 (D_{c,v_7}=170 m) and the second range (410 m) accounts for larger fields such as those of the sub-domain v_9 (D_{c,v_9}=370 m). Besides, the average of the spatial heterogeneity characteristics of the sub-domains are close to those computed at the image scale (Fig. 9).

Since the variogram provides the mean characteristics of spatial heterogeneity at the image scale, this information is sufficient to quantify globally the mean spatial heterogeneity of an image sub-domain. But the description of the local spatial variability may be limited. Other methods like wavelet analysis should be used to detect and quantify local variability and local length scales within the image.

6.3. Sufficient pixel size to capture the landscape length scales

The typical length scales of the landscapes, quantified in this work by the parameter D_c, may be used to compute on each scene the largest pixel size at which the major part of the spatial variability of the landscape is resolved. Shannon's theorem states that the proper sampling frequency of a signal must be higher than twice the maximal frequency of this signal (Shannon, 1948). We have seen that D_c is the distance separating the "equivalent independent data" if one assumes that they are arranged on a regular grid. Using Shannon's theorem, the spatial sampling frequency must then be larger than $2/D_c$. Hence, the pixel size must be smaller than $D_c/2$ to retain the major part of the NDVI spatial variability. Using this criterion on the landscapes under study, the range of the $D_c/2$ values is between 108 and 530 m, with an average of 324 m. Our results are limited by the number and the nature of the landscapes studied, but the minimum of the $D_c/2$ values computed on the 18 images of the VALERI database (108 m) is an indication of the upper limit of the sufficient pixel size to capture the major part of the spatial variability of the vegetation cover at the landscape level.

To limit the influence of spatial heterogeneity on non-linear estimation processes of land surface variables from remote sensing data, the proper pixel size must be small enough to capture the spatial variability of the data and minimize the spatial variability within the pixel. The parameter TH_v measures the loss of NDVI spatial variability at a given spatial resolution v with respect to its variability at 20 m spatial resolution. For most of the sites studied in this work, and especially for all the heterogeneous cropland sites, the loss of NDVI spatial variability at 100 m spatial resolution TH_{100} is less than 30% (Table 4). In addition, the sites for which TH_{100} is important are homogeneous sites at the landscape level and thus their intra-pixel heterogeneity $\gamma(v,v)$ is low at 100 m spatial resolution. Therefore, regarding the sites under study, the 100 m pixel size will reduce the bias generated by the intra-pixel spatial heterogeneity on non-linear estimation processes.

7. Conclusion

This work showed that modeling the variogram of high spatial resolution NDVI data is a powerful method to characterize and quantify the spatial heterogeneity of vegetation cover at the landscape level. The variogram sill σ^2 measures the landscape spatial variability. The image spatial structures are characterized by both the variogram ranges and the fractions of the total variance associated with each range. In addition, we introduced the concept of integral range which summarizes all structural parameters of the variogram model into a single characteristic area. Its square root is a weighted average of the several range parameters and quantifies the mean length scale of the data, i.e. the mean extent of the image spatial structures. The integral range is used as a yardstick to judge if the size of an image is large enough to measure properly the length scales of the data by the variogram. We propose that it must be smaller than 5% of the image surface. The square root of the integral range must thus be smaller than 671 m for a 3000 by 3000 m image.

The modeling of NDVI variogram for 18 contrasted landscapes highlights the influence of the land use on the spatial heterogeneity of vegetation cover at the landscape level. The most heterogeneous sites (σ^2 between 0.02 and 0.05) are cropland for which the field spatial structure explains the most important part (from 60% to 100%) of the NDVI spatial variability. Natural vegetation and forest sites are more homogeneous at the landscape level (σ^2 between 0.0001 and 0.02). However, their variability may be increased by the presence of singular objects with respect to the type of vegetation. The mean length scale of the landscapes varies between 216 and 1060 m. It results from several processes such as human activity, ecosystem functioning, or climate. Note that on some landscapes, the size of the image was too small to properly quantify its length scales. A 7000 by 7000 m extent would have been more appropriate for these cases.

Variogram modeling is an efficient approach to characterize the loss of spatial variability captured by the sensor as its spatial resolution decreases. A spatial structure cannot be resolved by the sensor when the pixel size is larger than its length scale. The theoretical dispersion variance, computed from the variogram model, quantifies the intra-pixel spatial heterogeneity. It increases rapidly with pixel size until this size is larger than the mean length scale of the data. It then tends asymptotically to the sill of the variogram σ^2. The dispersion variance at the sensor spatial resolution may be used as additional knowledge to correct non-linear estimation processes of land surface variables from remote sensing data. However, ways have to be found to get prior knowledge of this intra-pixel spatial heterogeneity metric without systematic concurrent high spatial resolution images that would make moderate spatial resolution images useless. A possible approach is to retrieve the intra-pixel spatial heterogeneity by using a temporal sampling or a spatial sampling per type of landscape of high spatial resolution data. To test this strategy, variogram modeling should be applied to a broader spatial and temporal database of high spatial resolution remote sensing data.

Finally, an upper limit of the sufficient pixel size to capture the major part of the spatial variability of the landscape vegetation cover is proposed from the mean length scale information provided by the variogram. From the analysis of 18 landscapes of the VALERI database, it is estimated to about 100 m. Since for all the heterogeneous landscapes the loss of NDVI spatial variability was small at this spatial resolution, the bias generated by the intra-pixel spatial heterogeneity on non-linear estimation processes will be reduced. However, this result is limited by the number and the nature of the landscapes analyzed. A more representative sampling of landscape types is required to refine the assessment of the sufficient pixel size. Since the variogram provides the mean characteristics of image spatial heterogeneity, its quantification of length scales can be coarse in some cases. Other tools, such as wavelet analysis, should be used to quantify finer local length scales in the image.

The definition of the optimal pixel size is not a trivial issue. It depends mainly on the objectives pursued, the objects observed and the retrieval techniques used. First, the pixel size must be large enough to be consistent with the object targeted and the retrieval technique considered. If the spatial resolution is too fine, spatial structures at small length scales may hamper the retrieval of the surface property. Further studies are required to estimate the lower limit of the proper pixel size to characterize the vegetation cover at the landscape level. Second, the pixel size must be small enough to capture the spatial variability of the data and minimize the intra-pixel spatial variability. The sufficient pixel size proposed in this study provides an indication of the upper limit of the proper pixel size to characterize the vegetation cover at the landscape level. The optimal pixel size should be chosen in between these two limits but additional factors, including technical and economic constraints, should be considered to define it for incoming earth observing missions.

Acknowledgements

This study was mainly completed under a PhD grant allocated to the first author by the french spatial agency CNES (Toulouse, France) and Alcatel Space Industry (Cannes, France). It also benefited from the availability of the VALERI data base under the responsibility of INRA Avignon (France) with funding mainly coming from CNES. Some writing of this

work was sponsored by NASA Grant EOS/03-0408-0637, with thanks to the program manager Dr. Wickland.

References

Atkinson, P. M. (1995). Defining an optimal size of support for remote sensing investigations. *IEEE Transactions on Geoscience and Remote Sensing*, *33*, 768–776.

Atkinson, P. M. (2001). Geostatistical regularization in remote sensing. In N. J. Tate, & P. M. Atkinson (Eds.), *Modelling Scale in Geographic Information Science* (pp. 237–260). New York: Wiley.

Baret, F., Weiss, M., Allard, D., Garrigues, S., Leroy, M., Jeanjean, H., Fernandes, R., Myneni, R.B., Morissette, J.T., Privette, J., Bohbot, H., Bosseno, R., Dedieu, G., Di Bella, C., Espana, M., Gond, V., Gu, X.F., Guyon, D., Lelong, C., Maisongrande, P., Mougin, E., Nilson, T., Veroustraete, F., Vintilla, R. (in press). VALERI: a network of sites and a methodology for the validation of medium spatial resolution land satellite product. *Remote Sensing of Environment*.

Bian, L. (1997). Multiscale nature of spatial data in scaling up environmental models. In D. A. Quattrochi, & M. F. Goodchild (Eds.), *Scale in remote sensing and GIS* (pp. 57–72). Boca Raton: Lewis Publishers.

Bierkens, M. F. P., Finke, P. A., & De Willigen, P. (2000). *Upscaling and downscaling methods for environmental research.* Dordrecht: Kluwer Academic Publishers. 204 pp.

Bruniquel-Pinel, V., & Gastellu-Etchegorry, J. -P. (1998). Sensitivity of texture of high resolution images of forest to biophysical and acquisition parameters. *Remote Sensing of Environment*, *65*, 61–85.

Cao, C., & Lam, N. S. (1997). Understanding the scale and resolution effects in remote sensing and GIS. In D. A. Quattrochi, & M. F. Goodchild (Eds.), *Scale in remote sensing and GIS* (pp. 57–72). Boca Raton: Lewis Publishers.

Carr, J. (1996). Spectral and textural classification of single and multiple band digital images. *Computers & Geosciences*, *22*, 849–865.

Chilès, J. -P., & Delfiner, P. (1999). *Geostatistics: modeling spatial uncertainy.* New-York: Wiley Inter-Science. 695 pp.

Collins, J. B., & Woodcock, C. E. (1999). Geostatistical estimation of resolution-dependent variance in remotely sensed images. *Photogrammetric Engineering and Remote Sensing*, *65*, 41–50.

Cosh, M. H., & Brutsaert, W. (2003). Microscale structural aspects of vegetation density variability. *Journal of Hydrology*, *276*, 128–136.

Cressie, N. (1985). Fitting variogram models by weighted least squares. *Mathematical Geology*, *17*, 563–586.

Csillag, F. (1997). Quadtrees: hierarchical multiresolution data structures for analysis of digital images. In D. A. Quattrochi, & M. F. Goodchild (Eds.), *Scale in remote sensing and GIS* (pp. 247–272). Boca Raton: Lewis Publishers.

Csillag, F., & Kabos, S. (1996). Hierarchical decomposition of variance with applications in environmental mapping based on satellite images. *Mathematical Geology*, *4*(28), 385–405.

Csillag, F., & Kabos, S. (2002). Wavelets, boundaries and the analysis of landscape pattern. *Ecoscience*, *9*, 177–190.

Curran, P. J. (1988). The semivariogram in remote sensing: An introduction. *Remote Sensing of Environment*, *24*, 493–507.

Curran, P. J., & Atkinson, P. M. (2002). Issues of scale and optimal pixel size. In A. Stein, F. Van Der Meer, & B. Gorte (Eds.), *Spatial statistics for remote sensing* (pp. 115–133). Dordrecht: Kluwer Academic Publishers.

De Cola, L. (1989). Fractal analysis of a classified landsat scene. *Photogrammetric Engineering and Remote Sensing*, *55*, 601–610.

De Cola, L. (1993). Multifractals in image processing and processing imaging. In N. S. -N. Lam, & L. De Cola (Eds.), *Fractals in geography* (pp. 282–304). Englewood Cliffs, NJ, U.S.A.: Prentice Hall.

Friedl, M. A. (1997). Examining the effects of sensor resolution and sub-pixel heterogeneity on spetral vegetation indices: Implications for biophysical modeling. In D. A. Quattrochi, & M. F. Goodchild (Eds.), *Scale in remote sensing and GIS* (pp. 113–140). Boca Raton: Lewis Publishers.

Gagalowicz, A. (1983). Vers un modèle de textures. PhD thesis, Université Pierre et Marie Curie, Paris VI. 351 pp.

Garrigues, S. (2004). Spatial heterogeneity from remote sensing observations of land surface: Characterization and effects on biophysical variable estimates. PhD thesis, Ecole Nationale Supérieure Agronomique de Rennes, France, 360 pp.

Garrigues, S., Allard, D., and Baret, F. (in press). Influence of the spatial heterogeneity on the non-linear estimation of Leaf Area Index from moderate resolution remote sensing data. *Remote Sensing of Environment.*

Haralick, R. M., & Shanmugan, K. S. (1974). Combined spectral and spatial processing of ERTS imagery data. *Remote Sensing of Environment*, *3*, 3–13.

Henebry, G. M. (1993). Detecting change in grasslands using measures of spatial dependence with landsat TM. *Remote Sensing of Environment*, *46*, 233–234.

Hu, Z., Chen, Y., & Islam, S. (1998). Multiscaling properties of soil moisture images and decomposition of large and small scale features using wavelet transforms. *International Journal of Remote Sensing*, *19* (13), 2451–2467.

Hu, Z., & Islam, S. (1997). A framework for analyzing and designing scale invariant remote sensing algorithms. *IEEE Transactions on Geoscience and Remote Sensing*, *35*, 747–755.

Jackson, R. D. (1983). Spectral indices in n-space. *Remote Sensing of Environment*, *13*, 409–421.

Journel, A. G., & Deutsch, C. V. (1993). Entropy and spatial disorder. *Mathematical Geology*, *25*(3), 329–355.

Julesz, B. (1962). Visual pattern discrimination. *Institute of Radio Engineers Transactions on Information Theory*, *8*, 84–92.

Jupp, D. L. B., Strahler, A. H., & Woodcock, C. E. (1988). Autocorrelation and regularization in digital images: I. Basic theory. *IEEE Transactions on Geoscience and Remote Sensing*, *26*, 463–473.

Jupp, D. L. B., Strahler, A. H., & Woodcock, C. E. (1988). Autocorrelation and regularization in digital images: II. Simple image models. *IEEE Transactions on Geoscience and Remote Sensing*, *27*, 247–258.

Kolasa, J., & Rollo, C. (1991). The heterogeneity of heterogeneity. In J. Kolasa, & S. T. A. Pickett (Eds.), *Ecological heterogeneity* (pp. 1–23). New York: Springer Verlag.

Lacaze, B., Rambal, S., & Winkel, T. (1994). Identifying spatial patterns of Mediterranean landscapes from geostatistical analysis of remotely-sensed data. *International Journal of Remote Sensing*, *15*(12), 2437–2450.

Lam, N. S. -N., & De Cola, L. (1993). *Fractals in geography.* Englewood Cliffs, NJ, U.S.A: Prentice Hall. 308 pp.

Lantuéjoul, C. (2002). *Geostatistical simulation: models and algorithms.* Berlin: Springer Verlag. 256 pp.

Lovejoy, S., Schertzer, D., Tessier, Y., & Gaonac'h, H. (2001). Multifractals and resolution-independent remote sensing algorithms: The example of ocean colour. *International Journal of Remote Sensing*, *22*(7), 1191–1234.

Mallat, S. (1999). *A wavelet tour of signal processing.* San Diego: Academic Press. 620 pp.

Mandelbrot, B. B. (1983). *The fractal geometry of nature.* New-York: W. H. Freeman 468 pp..

Marceau, D. J., Gratton, D. J., Fournier, R. A., & Fortin, J. -P. (1994). Remote sensing and the measurement of geographical entities in a forested environment: 2. The optimal spatial resolution. *Remote Sensing of Environment*, *49*, 105–117.

Matheron, G. (1965). *Les variables régionalisées et leur estimation.* Paris: Masson. 305 pp.

Morisette, J.T., Baret, F., Privette, J.L., Myneni, R.B., Nickeson, J., Garrigues, S., et al. (in press). Validation of global moderate-resolution LAI Products: a framework proposed within the CEOS Land Product Validation subgroup. *IEEE Transactions on Geoscience and Remote Sensing*.

Morisette, J. T., Privette, J. L., & Justice, C. O. (2002). A framework for the validation of MODIS land products. *Remote Sensing of Environment*, *83*(1–2), 77–96.

Myers, D. (1997). Statistical models for multiple-scaled analysis. In D. A. Quattrochi, & M. F. Goodchild (Eds.), *Scale in remote sensing and GIS* (pp. 273–294). Boca Raton: Lewis Publishers.

O'Neill, R. V., Gardner, R. H., Milne, B., Turner, M. G., & Jackson, B. (1991). Heterogeneity and spatial hierarchies. In J. Kolasa, & S. T. A. Pickett (Eds.), *Ecological heterogeneity* (pp. 85–96). New York: Springer Verlag.

Oliver, M. A. (2001). Spatial scale variation in environmental properties. In N. J. Tate, & P. M. Atkinson (Eds.), *Modelling scale in geographic information science* (pp. 193–219). New York: Wiley.

Puech, C. (1994). Thresholds of homogeneity in targets in the landscape. Relationship with remote sensing. *International Journal of Remote Sensing*, *15*(12), 2421–2435.

Quattrochi, D. A., & Goodchild, M. F. (1997). *Scale in remote sensing and GIS.* Boca Raton: Lewis Publishers. 432 pp.

Raffy, A. M. (1994). Change of scale theory: a capital challenge for space observation of earth. *International Journal of Remote Sensing*, *15*, 2353–2357.

Rahman, A. F., Gamon, J. A., Sims, D. A., & Schmidts, M. (2003). Optimum pixel size for hyperspectral studies of ecosystem function in southern California chaparral and grassland. *Remote Sensing of Environment*, *84*(2), 192–207.

Ramstein, G., & Raffy, M. (1989). Analysis of the structure of remotely-sensed images. *International Journal of Remote sensing*, *10*, 1019–1073.

Serra, J. (1982). *Image analysis and mathematical morphology.*London, New-York: Academic Press. 600 pp.

Shannon, C.E. (1948). A mathematical theory of communication. Bell System Technical Journal, 23, 379–423 and 623–656.

St-Onge, B. A., & Cavayas, F. (1995). Estimating forest stand structure from high-resolution imagery using the directional variogram. *International Journal of Remote Sensing*, *16*(11), 1999–2001.

Stein, A., & Ettema, C. (2003). An overview of spatial sampling procedures and experimental design of spatial studies for ecosystem comparisons. *Agriculture, Ecosystems and Environment*, *94*, 31–47.

Tian, Y., Woodcock, C. E., Wang, Y., Privette, J. L., Shabanov, N. V., Zhou, L., et al. (2002). Multiscale analysis and validation of the MODIS LAI product. I. Uncertainty assessment. *Remote Sensing of Environment*, *83*, 414–430.

Wackernagel, H. (2003). *Multivariate geostatistics: An introduction with applications.* Berlin: Springer. 387 pp.

Walsh, S. J., Moody, A., Allen, T. R., & Brown, D. G. (1997). Scale dependence of NDVI. In D. A. Quattrochi, & M. F. Goodchild (Eds.), *Scale in remote sensing and GIS* (pp. 27–56). Boca Raton: Lewis Publishers.

Weiss, M., Baret, F., Myneni, R. B., Pragnère, A., & Knyazikhin, Y. (2000). Investigation of a model inversion technique to estimate canopy biophysical variables from spectral and directional reflectance data. *Agronomie*, *20*, 3–22.

Woodcock, C. E., & Harward, V. J. (1992). Nested-hierarchical scene models and image segmentation. *International Journal of Remote Sensing*, *13*(16), 3167–3187.

Woodcock, C. E., & Strahler, A. H. (1987). The factor of scale in remote sensing. *Remote Sensing of Environment*, *21*, 311–332.

Woodcock, C. E., Strahler, A. H., & Jupp, D. L. B. (1988). The use of variograms in remote sensing: A/ scene models and simulated images. *Remote Sensing of Environment*, *25*, 323–348.

Woodcock, C. E., Strahler, A. H., & Jupp, D. L. B. (1988). The use of variograms in remote sensing: B/ real digital images. *Remote Sensing of Environment*, *25*, 349–379.